



Assessment of metal contamination and the associated human health risk from dustfall deposition: a study in a mid-sized town in India

Neha Rani¹ · Bhamidipati S. Sastry¹ · Kaushik Dey¹

Received: 14 February 2019 / Accepted: 21 May 2019 / Published online: 12 June 2019
© Springer-Verlag GmbH Germany, part of Springer Nature 2019

Abstract

It is evident from the past studies that dust fallout is a severe concern due to its impact to urban air quality and public health. This study mainly examines the spatial and seasonal variation of dustfall at ambient levels and chemical characterization of its insoluble fraction for Kharagpur Town, India. Dustfall samples were collected monthly for 1 year (July 2014 to June 2015) from four sampling sites. The results showed that the maximum dustfall deposition is found during summer (March to June) and in the range of 2.01 ± 0.36 to 15.74 ± 3.83 ton km^{-2} month⁻¹, and minimum deposition is during monsoon season (July to October) in the range of 0.42 ± 0.72 to 7.38 ± 5.8 ton km^{-2} month⁻¹. Selected metals like Sc, V, Cr, Co, Ni, Zn, Y, Zr, Ce, Hf, and Pb were analyzed using the high-resolution inductively coupled mass spectrometer (HR-ICP-MS) technique, and the contamination level of heavy metals was assessed using the geoaccumulation index (I_{geo}) and enrichment factor (EF). To estimate the sources for the metallic contaminants, principal component analysis (PCA) was conducted. The US EPA health risk assessment model was applied to determine the hazard index and hazard quotient values. The results show the significant level of enrichment for Pb (EF = 41.79) and Cr (EF = 4.39). The I_{geo} values point out moderate contamination by Pb ($I_{\text{geo}} = 2.01$) and Cr ($I_{\text{geo}} = 1.6$) in Kharagpur Town. This study suggests that in the context of noncancer risk of heavy metals as determined by the hazard index (HI) and hazard quotient (HQ) values, ingestion is the main source of exposure to dust in adults and children followed by dermal contact. Considering the inhalation route, carcinogenic risk level of Cr, Co, and Ni for adults and children is lower than the EPA's safe limit (10^{-6} to 10^{-4}), indicating that cancer risk of these metals due to exposure to dustfall in Kharagpur is negligible.

Keywords Heavy metal · Dustfall · Principal component analysis · Health risk · Hazard index

Introduction

It is evident from the past studies that environmental degradation is the consequence of accelerated and unmethodical growth of several industries evolved for the development of a city or town (Kumar 2013; Holnicki et al. 2017). Soil

erosion causes the generation of natural dust particles, whereas human activities such as traffic, industrial emissions, and construction or demolition of buildings contribute a large portion of the anthropogenic dust in to the environment (Adachi and Tainosho 2005). Besides the components of natural earth crust, dust generated from the human-made activities is highly responsible to add contaminants with significant level of metal concentrations from atmosphere to topsoil by the process of interception, sedimentation, and impaction (Li et al. 2001). Due to the occurrence of significant level of contamination and its regular exchange with atmosphere as well as other mediums through resuspension and deposition, urban road dust is considered as a “sink and source” of pollutants (Moreno et al. 2013). Thus, the main reason of metal contamination is atmospheric pollution, and furthermore, the topsoil and roadside dust adjacent to industrial and urban area is the true representative of metal pollution. Road dust is an indicator of heavy metal contamination from atmospheric deposition

Responsible editor: Philippe Garrigues

Electronic supplementary material The online version of this article (<https://doi.org/10.1007/s11356-019-05539-7>) contains supplementary material, which is available to authorized users.

✉ Bhamidipati S. Sastry
bssastry@mining.iitkgp.ac.in

¹ Department of Mining Engineering, Indian Institute of Technology Kharagpur, Kharagpur, West Bengal 721302, India

due to its significant contribution to environmental pollution. Heavy metals are cytotoxic due to their impacts on cellular level of plants, animals, and human beings. They are persistent with tendency to accumulate within living organism and, therefore, known as priority environmental pollutants (Zhang et al. 2017). The toxicity of the metal-loaded dust spread to the aquatic system by urban discharge (Zhao et al. 2010; Kong et al. 2012) and the atmosphere as a resuspension (Ferreira-Baptista and De Miguel 2005). Thus, heavy metal pollution in any form can lead to the permanent harm to the environment and increase the rate of mortality in human beings (Adamiec et al. 2016; Khorshid and Thiele-Bruhn 2016). Therefore, it is imperative to know clearly about metal contamination such as their sources and associated degree of toxicity (Trujillo-González et al. 2016; Li et al. 2017). Additionally, the human body may expose to dust using the three main pathways, e.g., inhalation of dust particles by mouth and nose, through direct ingestion of dust, and dermal absorption. Metal-laden dust can be easily deposited in the adipose tissue or can circulate throughout the body, causing serious damage to the nervous system and internal organs (Soltani et al. 2015; Gope et al. 2017) due to its toxic property and nonbiodegradability (Tang et al. 2013). The past studies revealed that the ingestion rate of dust in adults is up to 100 mg dust day⁻¹ in dusty environments (Leung et al. 2008). It is also noted in the previous studies that dust exposure rate in children is high as compared with adults because of tendency of touching and mouthing of dust-contaminated objects (Kurt-Karakus 2012). The carcinogenic effect of metals causes deadly health hazards like lung cancer and other respiratory diseases (Green and Armstrong 2003; Qian et al. 2007). Therefore, many studies have been conducted around the world to investigate extensively the components of urban road dust and its adverse health hazards to protect the ecological environment and public health (Li et al. 2001; Banerjee 2003; Yongming et al. 2006; Al-Khashman 2007; Han et al. 2008; Faiz et al. 2009; Lu et al. 2009a, b, 2010; Atiemo et al. 2011). The US EPA health risk assessment model is proved as a widely used model to determine the quantitative risks of heavy metal exposure (US EPA 1989). Several studies about heavy metal concentration level, distribution pattern, pollution indices, and health risk assessment have been conducted in the past and reported very well in literature (Apeagyei et al. 2011), but majority of them were carried out in developed countries or the big cities of developing countries (Banerjee 2003; Yongming et al. 2006; Shi et al. 2011; Nazzal et al. 2014; Tang et al. 2013). There are many fast growing medium and small cities or towns, untouched or with less information about heavy metal contamination, and need to pay serious attention (Lu et al. 2014). The population density and industrial activities are different in small cities or developing countries as compared with developed countries or the megacities. Therefore, they may have a great influence on the findings of individual studies. The

medium and small industrial cities might have more serious environmental issues as compared with megacities, owing to poor environmental protection strategies and inadequate pollution treatment techniques (Lu et al. 2014).

Atmospheric dustfall is considered as one of the important measures of urban environmental monitoring to indicate the impact of environmental particulate pollution (Guo et al. 2006; Wang et al. 2015). The dustfall measurement as per American Society for Testing and Materials (ASTM D 1739-98 2004) is a widely used technique to assess the concentration of settled dust in the units of ton km⁻² month⁻¹. Some studies that have been conducted in India discussed the severe dispersion and fallout of fugitive dust and its significant association with health disorders particularly bronchial ailments. According to those studies, large-sized particles of dust fallout are the major cause of asthma, whereas small-sized particles cause inner respiratory disorders (Balakrishna and Pervez 2009). Earlier studies on dust fallout has described greatly about the regional and continental transportation of atmospheric dust fallout and the influence of local sources of emissions, meteorology, topography, and other physiographic factors on degree of spatiotemporal variations in coarser particulates compared with fine ones (Freiman et al. 2006; Balakrishna and Pervez 2009; Gurugubelli et al. 2013). Thus, it is essential to study the spatial and temporal deposition of dust fallout pattern in urban centers and identification of airborne dust-carried elements. Furthermore, chemical characterization and source identification of dustfall (for local and remote sources) can produce valuable information to conduct atmospheric pollution assessment.

Geoaccumulation index (I_{geo}) introduced by Muller (1969) is an assessment method to determine the contamination of heavy metals in urban road dusts, urban soils, and agriculture soils and extensively employed in European trace metal studies since the late 1960s (Wei and Yang 2010). Enrichment factor (EF) is widely studied to apportion the local sources by identifying anthropogenic activities in global element cycles (Khuzestani and Souri 2013; Wang et al. 2015; Luo et al. 2016). The EF value of an element in a certain material signifies the level of enrichment of that investigated element in that material. The limitation of EF in identifying the sources (Reimann and Caritat 2000) can be reduced by conducting simultaneously a multivariate numerical technique like principal component analysis (PCA).

Kharagpur, a mid-sized town in west Bengal, is undergoing fast population growth and industrial development in the last decades. The town is experiencing higher level particulate pollution, due to heavy traffic congestion, small-scale industrial development, railway yard and workshops, and large-scale construction projects. Even though, there is no known work conducted on air quality of Kharagpur Town and so no such defined origin has been reported earlier in any literature, therefore, traffic generated dust is assumed to be one of the reasons for particulate pollution in Kharagpur. In this study, the seasonal and spatial variation of dustfall deposition rate and its insoluble fraction was studied for

Kharagpur Town with the help of dustfall jars placed for 1 year. Additionally, a soil sampling was also conducted from an unpolluted area near the study site to know the background information about the geochemistry of the surrounding soil. The dustfall samples were grouped into a total of 12 samples and then investigated for elemental concentration using the HR-ICP-MS technique. The results were analyzed using the techniques of contamination assessment methods (I_{geo} and EF), PCA, and health risk indices like hazard quotient (HQ) and hazard index (HI).

Details of the study area

Sampling area description

Kharagpur (22°30' N, 87°20' E) is a mid-sized town in Gangetic West Bengal with a population of 207,604 and annual rainfall of about 1400 mm. At present, small-scale industries such as sponge iron plants (Sponge Iron Plant), thermal power plants (Bengal Energy Ltd.), cement rehandling, vehicular traffic, and semiurban roads are the main sources contributing to dust on the sampling site. Out of the four locations, two of the sampling sites are on the academic campus of IIT Kharagpur (Loc. 1 and Loc. 2), and two within the town of Kharagpur (Loc. 3 and Loc. 4) (Fig. 1). The abovementioned locations are selected in according to local meteorology, type of human activities, and proper installation of sampling jars.

Loc. 1 (Kaju Bagan) is mainly a residential area situated inside the campus and consists of faculty quarters. The area is completely a residential area surrounded with residential buildings and green vegetation cover. Loc. 2 is a traffic area situated near to the main gate of campus and is exposed to the local and moderate traffic of the campus. Loc. 3 is an area outside the campus and near to a petrol station, affected by the dust generated by busy traffic and vehicular movement. Loc. 4 is a residential area outside the campus but situated roadside, affected by vehicular traffic. The geology of the study area is characterized by the presence of lateritic soil associated with Tertiary sedimentaries, which confirms the presence of sodium, iron, and aluminum oxide in the subsurface strata (Ghosh and Guchhait 2015). Geological succession indicates that during the Pre-Cambrian age, the region contains phyllites, micaschists, quartzite, hornblende schists, dolerite, etc. During the Quaternary age in Pleistocene formation, the area covered with laterites, brown sandy clay, brown to reddish brown sand, and molted and variegated clays coarse to gritty ferruginous sand (GSI 1983).

Meteorology

It is marked from the previous studies that the wind direction and mean wind speed play a significant role to study the transport and dispersion of pollutants (Ziomas et al. 1995). The Kharagpur Town has a monthly wind speed ranged from 0.65

to 15.4 m s⁻¹ with average of 2.24 m s⁻¹. During winter season, 27% was the maximum calm condition (< 1 m/s) (Hao et al. 2000; Tiwari et al. 2018). The calm percentages of wind during monsoon and summer were 20.5% and 12.2%, respectively. The rainfall (precipitation) of approximately 1308 mm was reported in the year of June 2014 to June 2015 (study time) for the Kharagpur Town with 24% (314.4 mm) of the total rainfall occurred in July. Rainy season covered 66% of the total rainfall with relative humidity ranged from 80 to 95%. During winter and summer seasons, relative humidity of Kharagpur Town recorded from 65 to 71% and 58 to 92%, respectively. The average temperature ranged from 27.7 to 35.6 °C in summer. Figure 2 demonstrates wind rose plot for Kharagpur Town with the help of data collected from Indian Meteorological Department (IMD), Pune. Seasonal and annual wind rose diagrams were generated by using “openair” package in R (version 3.4.0) and presented in Fig. 2a–d to examine the surface wind conditions (direction and speed) from measurement data at Kharagpur during different seasons. Southwesterly winds were predominant during summer followed by rainy season, also the most prevailing wind throughout the year. After southwesterly winds, the most common were north and northeasterly winds, which were experienced more often from November to February. The average calm percentage recorded to be 19.6%.

Materials and methods

Sample collection

Dustfall samples were collected at the end of each month for a period of 1 year from June 2014 to July 2015 from the four locations. According to standard test method for collection and measurement of dustfall ASTM (D 1739-98 2004), borosilicate jars of diameter 6 in. and height 12 in. were mounted at the height of 5 ft from the ground for dust collection. The jar was guarded with a wind shield and a wire mesh to avoid birds. One liter of double-distilled water was poured into the jar to retain the dust falling in the jar. A small amount of copper sulfate (0.02 N) solution was added to the jar to avoid algal growth. The jar was inspected each week either to replenish evaporated water or to remove excess water resulting from rains. The dust was captured on the Whatman 42 ash less filter paper by the method of vacuum filtration of the water in the jar to examine the composition of the insoluble matter. After filtration, the dust-loaded filter paper was left for drying in a hot air oven at 108 °C for 2.5 h for moisture removal. After 2.5 h of drying, the filter paper was taken out from the oven and placed in a desiccator till it achieved normal ambient temperature. The insoluble portion of the sample was estimated by a well-known method used by Norela et al. (2009), by different parameters like the area of the dustfall jar opening mouth and number of days (in 1 month) weight differences of filter papers.

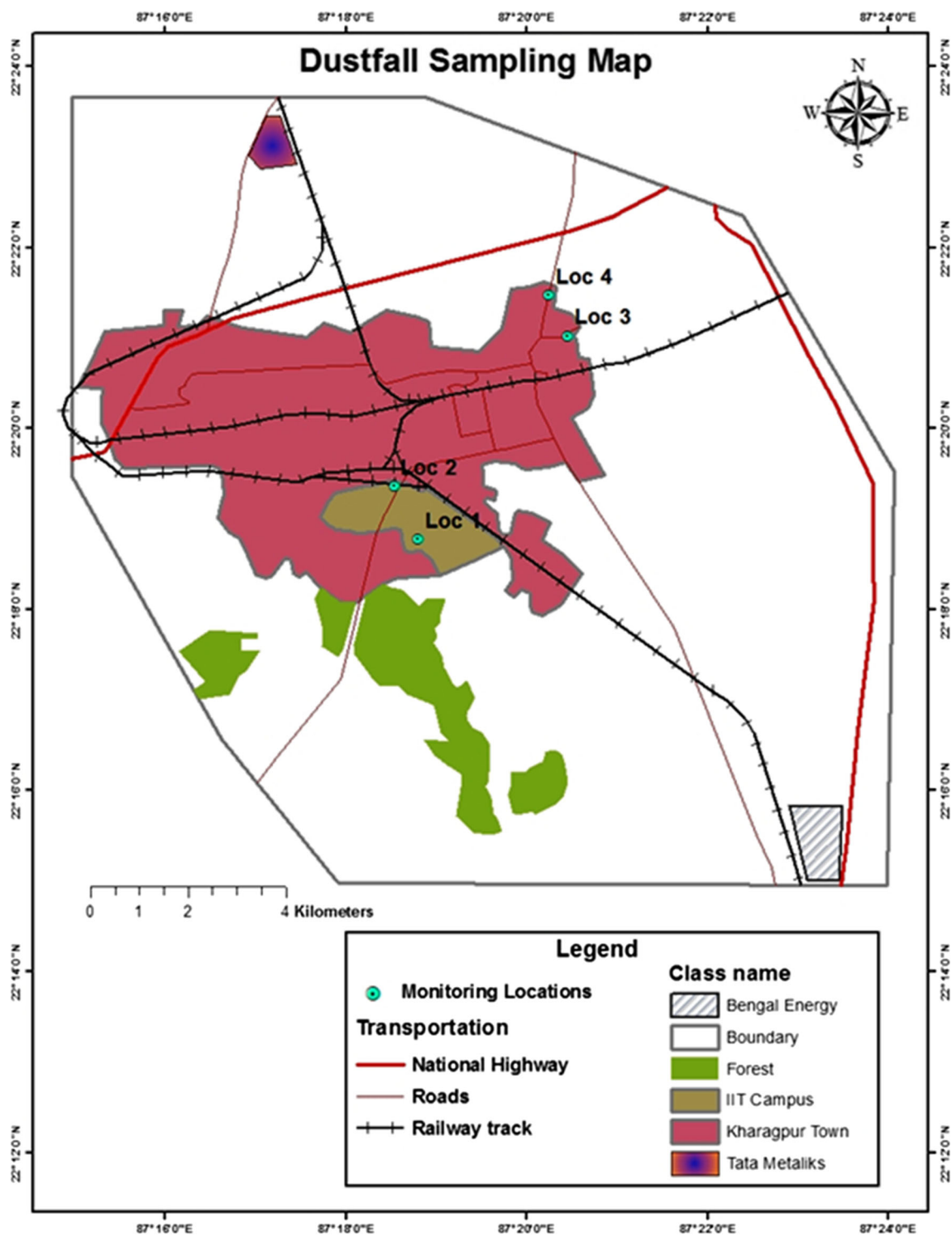


Fig. 1 Study area and sampling locations of Kharagpur Town

The final dried dust sample was collected in a small air tight plastic container and stored at room temperature for the analysis. The sampling has been continued for 1 year, and a total of 48 samples from 4 sites have been collected. The rate of deposition was determined using the following equation (Katz 1969) and expressed in $\text{ton km}^{-2} \text{month}^{-1}$.

$$\text{Dustfall rate } (\text{ton km}^{-2} \text{month}^{-1}) = \frac{W}{a} \times \frac{30}{t} \quad (1)$$

where W is the weight analyzed (g), a is the open area of sampling container at top (cm^2), and t is the time of exposure (days).

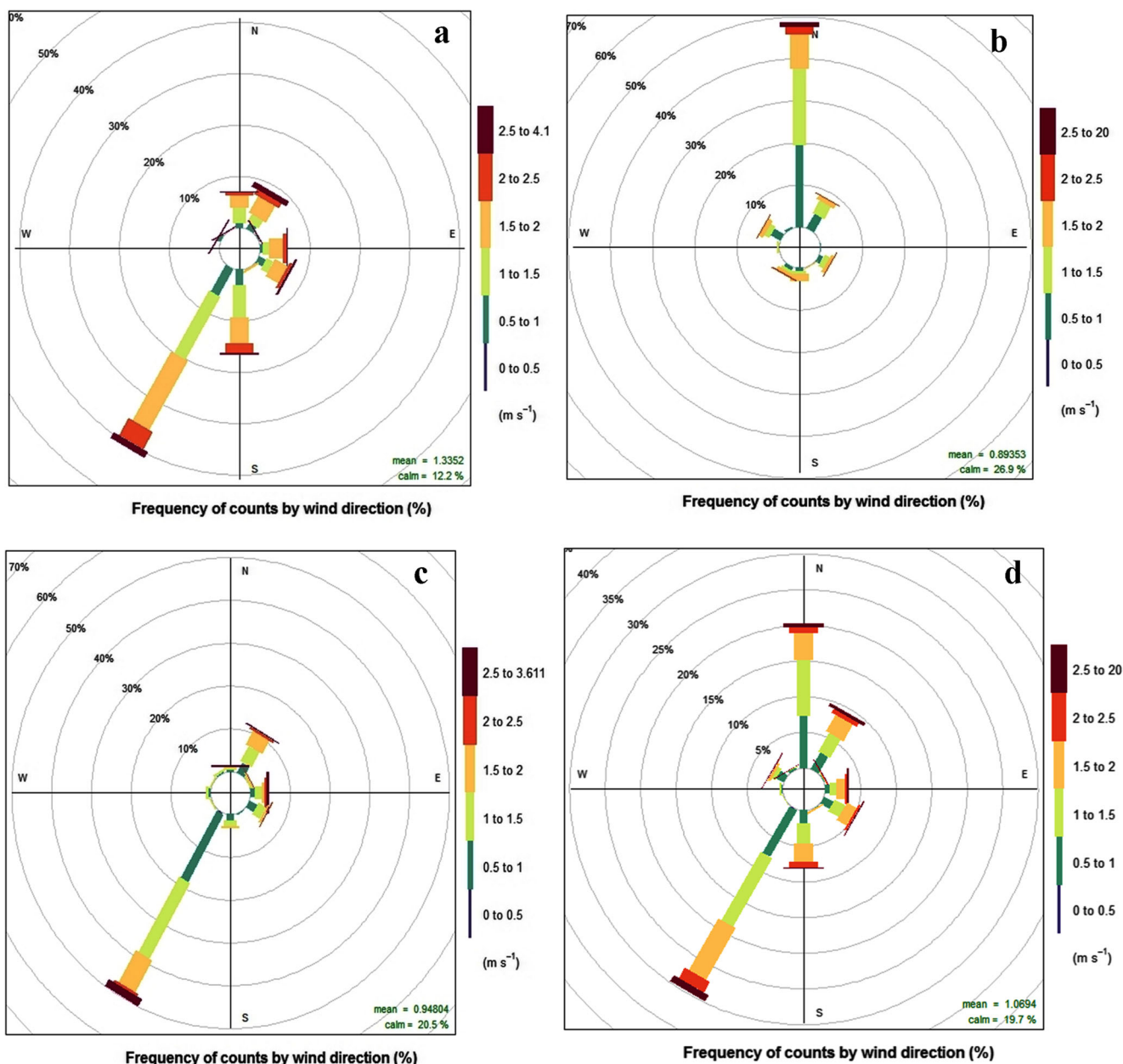


Fig. 2 Wind rose plots of Kharagpur Town developed from June 2014 to July 2015. a Summer. b Winter. c Monsoon. d Annual

Soil sample collection

A soil sample was collected from an unpolluted area near the town in order to get information about the background geochemistry of the soil. A sample to a depth of 15–20 cm was collected using a stainless steel shovel and dried at 37–40 °C for 48 h followed by sieving to 2-mm sieve prior to analysis.

Sample preparation

After determining mass, all the dustfall samples were processed for elemental analysis using the HR-ICP-MS technique. As the mass of dust collected for each month was small for HR-ICP-

MS, samples of four consecutive months were combined. A total of twelve samples were thus obtained from the four locations, each location providing three samples over the year. Before experimenting, all glassware was drenched in 10% (v/v) nitric acid for overnight and washed thoroughly with ultrapure water to protect them from contamination of metals. The extraction of heavy metals in dustfall samples was conducted by dissolving the 0.05 g of each homogenized sample in reagent grade HF: HNO₃ acid mixture poured in 25 ml of Savillex® screwtop vessels. An acid mixture of HF and HNO₃ in the proportion of 7:3 was added to each Savillex containing sample. Then, 5 ml of 1 ng ml⁻¹ ¹⁰³Rh solution of an internal standard was added to each Savillex® vessel. After thorough spinning, the vessels

were closed tightly with the help of lid and placed on a hot plate at $\sim 140\text{ }^\circ\text{C}$ for 48 h for digestion. Subsequently, the content of the vessels was undergone evaporation at $200\text{ }^\circ\text{C}$ to near dryness followed by adding few drops of HClO_4 to remove HF completely from the mixture. After evaporation, the dried residue left was dissolved with the help of 10 ml of 1:1 HNO_3 and made the final volume up to 250 ml by adding Milli-Q® deionized water (18 M Ω). The final solution was kept ready in sample bottles in the refrigerator for further analysis.

Analytical aspects

The elements selected in the present study are based on their abundance in soil (Al, Sc, Ni, Y, Ce, Zr, etc.) and those assumed to be mainly resulting from anthropogenic activities (Zn, Co, Cr, Pb, etc.) such as traffic and biomass burning (Church and Scudlark 1998). Therefore, this study reports the concentration of Sc, V, Cr, Co, Ni, Zn, Y, Zr, Ce, Hf, and Pb determined by using HR-ICP-MS (Nu Instruments Attom, UK) at CSIR-NGRI, Hyderabad, India. The operation was done in jump–wobble mode at moderate resolution to achieve maximum accuracy for all the desired elements. To minimize operational and handling errors, reference samples of NIST 1648 (National Institute of Standards and Technology, USA) along with couple of procedural blanks were also prepared by using same protocol mentioned above. Internal standards (Rh, Ge, Sc, Tb, Lu) were also used to check the sensitivity and stability of the instrument used. A 5-point calibration was performed for all the tested elements, and the regression coefficients better than 0.9996 were achieved. The relative standard deviation (RSD) counts per second (CPS) and mean values of these elements were also calculated, and RSD was ranging from 0.69 to 1.56% with a mean value of 1.04%. The operating condition of the instrument and the concentration of heavy metals obtained in certified reference material are given in Table S1 and S2 in Supplementary data.

Contamination assessment methods

The techniques of I_{geo} and EF were used to determine the intensity of heavy metal pollution of the examined environment. The techniques require a comparison of the observed heavy metal concentration with the background concentration (Loska et al. 2004). Taylor and McLennan (1985) suggested the use of upper continental crust (UCC) values as a background value for the estimation of I_{geo} . The I_{geo} was computed by using the following equation.

$$I_{\text{geo}} = \log_2 \frac{C_n}{1.5B_n} \quad (2)$$

where C_n denotes the measured concentration of the examined element (n) in the sample (atmospheric dustfall), and B_n is the background value (UCC) of the element (n). There is a factor of

constant value (1.5) called background matrix correction factor used in the above equation to reduce the effect of lithogenic variability (Loska et al. 2004). According to Muller 1981, I_{geo} has seven levels of contamination starting from 0 (uncontaminated) to 6 (extremely contaminated) as follows: $I_{\text{geo}} \leq 0$ practically uncontaminated; $0 < I_{\text{geo}} \leq 1$ uncontaminated to moderately contaminated; $1 < I_{\text{geo}} < 2$ moderately contaminated; $2 < I_{\text{geo}} < 3$ moderately to heavily contaminated; $3 < I_{\text{geo}} < 4$ heavily contaminated; $4 < I_{\text{geo}} < 5$ heavily to extremely contaminated; and $5 < I_{\text{geo}}$ extremely contaminated.

EF of an element in the studied samples was based on standardization of a tested element against a reference element (e.g., Al, Fe, Ti, Sc, and Mn) which is generated by anthropogenic sources (Reimann and Caritat 2000). The EF value was calculated using the formula modified by Loska et al. (2004) which in turn was based on the equation suggested by Buat-Menard and Chesselet (1979).

$$EF = \frac{[C_n(\text{sample})/C_{\text{ref}}(\text{sample})]}{[B_n(\text{background})/B_{\text{ref}}(\text{background})]} \quad (3)$$

where C_n (sample) is the content of the element of interest in the examined environment (dust), C_{ref} (sample) is the content of the reference element in the examined environment, and B_n (background) and B_{ref} (background) represent the concentrations of the element of interest and the reference element in the UCC. The enrichment factor is a tool, mostly used to recognize the sources of elements in terms of natural or anthropogenic origin and extension of human contribution (Mun'im Mohd Han et al. 2014; Norouzi et al. 2017). In this study, Sc is selected as the reference element. There are five contamination categories of EF suggested by Sutherland (2000) which as follows: $EF < 2$ deficiency to minimal enrichment; $EF = 2–5$ moderate enrichment; $EF = 5–20$ significant enrichment; $EF = 20–40$ very high enrichment; and $EF > 40$ extremely high enrichment.

Statistical analysis

Table 3 represents the basic statistics of metals studied in dustfall samples. The acquired data set was subjected to principal component analysis (PCA) to determine the possible factors contributing towards the metal concentrations and to identify metals having common origin. PCA is widely used in metal pollution studies to find the associations and sources of trace elements and air pollutants (Manno et al. 2006; Shah and Shaheen 2007; Ragosta et al. 2008). It can interpret variance in a given data set regarding a minimum number of significant components by extracting the eigenvectors and eigenvalues from the correlation matrix. The SPSS 20.0 software package was applied to perform the statistical analyses of the data. In this study, correlation was checked for the dustfall data, and exponential regression analysis was applied between dustfall

locations and rainfall data. A two-way analysis of variance (ANOVA) was also carried out in Microsoft-Excel.

Risk assessment model

The risk of heavy metals from the dustfall samples was assessed by using the US EPA health risk assessment model. The chemical daily intake (CDI) through three major pathways, namely, ingestion (CDI_{ing}), inhalation through nose and mouth (CDI_{inh}), and dermal contact (CDI_{dermal}), were examined to evaluate the noncarcinogenic risk and carcinogenic risk to population in Kharagpur Town. The CDI through each of the three pathways was calculated (US EPA 1989, 1996; Ferreira-Baptista and De Miguel 2005; Li et al. 2017) separately for children and adults by using the formulas listed below.

$$CDI_{ing} = C \times \frac{R_{ing} \times EF \times ED}{BW \times AT} \times 10^{-6} \tag{4}$$

$$CDI_{inh} = C \times \frac{R_{inh} \times EF \times ED}{PEF \times BW \times AT} \tag{5}$$

$$CDI_{dermal} = C \times \frac{SL \times SA \times ABS \times EF \times ED}{BW \times AT} \times 10^{-6} \tag{6}$$

In the above expressions, CDI is expressed in mg kg⁻¹ day⁻¹. R_{ing} is the ingestion rate at 100 mg dust day⁻¹ for adults and 200 mg dust day⁻¹ for children (1–6 years) (US EPA 2011). R_{inh} is the inhalation rate at 20 m³ day⁻¹ for adults and 7.6 m³ day⁻¹ for children (Van den Berg 1994). EF is the exposure frequency (365 days in a year). ED is the exposure duration taken 24 years for adults and 6 years for children (US EPA 2001). SA is the skin area considered as 5700 cm² for adults and 2800 cm² for children (US EPA 2001). SL is the skin adherence factor at 0.7 mg cm⁻² h⁻¹ for adults and 0.2 mg cm⁻² h⁻¹ for children (US EPA 2002b). ABS is the dermal exposure factor (unit less) taken as 0.001 for all elements, while PEF is the particle emission factor taken at 1.36 × 10⁹ m³ kg⁻¹ (US EPA 2001). BW is the average body weight taken as 70 kg for adults and 15 kg for children (US EPA 1989). AT (averaging time) is taken as the exposure duration in days (ED × 365 days) for noncarcinogenic risk and carcinogens. AT is taken as 70 × 365 = 25,550 days (Kurt-Karakus 2012).

C is the upper limit of the 95% confidence interval of the mean for the metals expressed in mg kg⁻¹. It is considered to yield an estimate of the “reasonable maximum exposure” (US EPA 1989; Zheng et al. 2010; Hu et al. 2011). For small sample sizes, as in the present case, the suggested procedure of determining the 95% upper confidence limit is given by the US EPA (2002a) and Kurt-Karakus (2012). As per this, C is calculated as follows:

$$C = \bar{X} + \left[Z_{\alpha} + \frac{\beta}{6\sqrt{n}} (1 + 2Z_{\alpha}^2) \right] \frac{STD}{\sqrt{n}} \tag{7}$$

In the above equation, STD is the standard deviation, \bar{X} is the arithmetic mean, β is the skewness, n is the number of samples, and Z_α for standard normal distribution at 95% confidence level is 1.645.

The CDI values were used to determine the quantified noncancer risk for each exposure pathway. The procedure adopted was based on estimating hazard quotient (HQ) for each metal considered. The hazard index (HI) for a given pathway is the sum of the HQ values. If the value of HI is less than one, there is no significant risk of noncarcinogenic effect. The probability of the noncarcinogenic risk increases as the HI values exceed one (US EPA 2001). Carcinogenic risk is defined as the probability of an individual developing any cancer from a lifetime exposure to carcinogenic hazards. The potential human carcinogenic risk associated with chemical exposure is expressed regarding an increased probability of developing cancer during a person’s lifetime, and acceptable or tolerable risk for regulatory purpose is given in the range of 1 × 10⁻⁶ to 1 × 10⁻⁴ (Ferreira-Baptista and De Miguel 2005). These values indicate an increased cancer risk of one in 1,000,000 to one in 10,000 people developing cancer (Lu et al. 2014). The potential carcinogenic and noncarcinogenic risks of the individual metals were calculated by using the following equations. (US EPA 2007; Kurt-Karakus 2012):

$$\text{Carcinogenic Risk} = CDI_{ing/inh/dermal} \times BAF \times SLF \tag{8}$$

$$\text{Hazard quotient (HQ)} = \frac{(CDI_{ing/inh/dermal} \times BAF)}{B_f D} \tag{9}$$

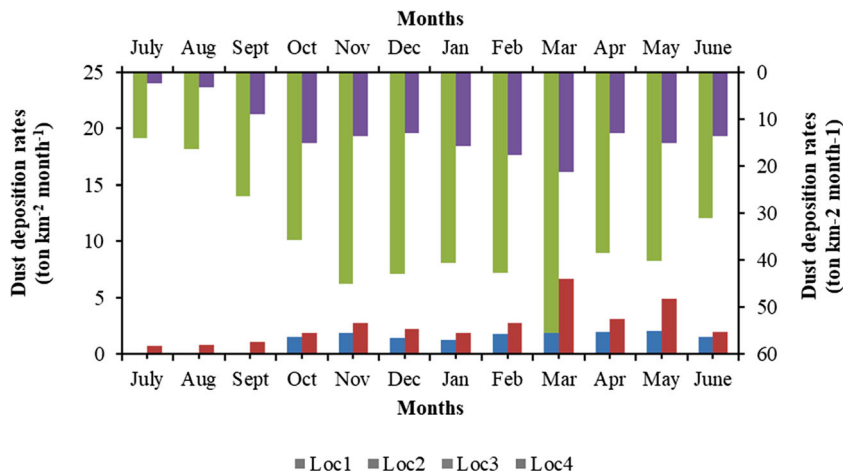
In the above equations, R_fD refers to the reference dose for all the pathways adopted from the US EPA (2010). BAF is the ratio of the metal contents that is bioavailable to the total content in the dust. For carcinogens, the cancer slope factor (SLF) for inhalation was used to produce a level of cancer risk for Co, Cr, and Ni (Lu et al. 2014). The BAF values for the street dust reported by Hu et al. (2011) were considered in the present study.

Results

Seasonal variation in dustfall

The average monthly variation in the dustfall deposition rate from July 2014 to June 2015 is represented in Fig. 3. The highest level of dustfall is obtained during summer season and reached from 2.01 ± 0.36 to 15.74 ± 3.83 ton km⁻² month⁻¹ due to high wind and low humidity as compared with winter and monsoon. Summer season is characterized by high temperature and low humidity with dusty winds attribute to surface erosion, and consequently, resuspension of dust increases the rate of dust deposition. The lowest values were observed during monsoon and ranged from 0.42 ± 0.72 to 7.38 ± 5.8 ton km⁻² month⁻¹. During

Fig. 3 Monthly variation (from July 2014 to June 2015) in dustfall deposition in Kharagpur Town, India



rainy season, heavy rain causes the washout of dust from the atmosphere and gives rise to the lowest level of deposition. Chate and Pranesha (2004) stated in their study about the removal of aerosol particles by falling raindrops with the help of some processes like Brownian and turbulent shear diffusion, thermophoresis, inertial impaction, electric charge effects, and diffusiophoresis. The moderate values were observed during winter months with a range of 1.60 ± 0.28 to $14.98 \pm 2.19 \text{ ton km}^{-2} \text{ month}^{-1}$. These findings could be attributed to the low surface temperature, wind speed, and high frequency of calm condition of wind (specially found during winter season) which lead to thermal inversions (Lyons and Scott 1990). ANOVA was conducted to compare the means of dustfall deposition rates between sites and seasons. The results obtained from two-way ANOVA are presented in Table 1. The mean dustfall concentration at different seasons and locations is found significantly different at $p < 0.05$.

Spatial variation in dustfall

From one-way ANOVA test, it is cleared that spatial variations are significant at $p < 0.05$. Figure 3 shows the amount of dust received among the four locations, and it was the highest ($55.51 \pm 12 \text{ ton km}^{-2} \text{ month}^{-1}$) in March at Loc. 3 situated near a petrol station and influenced by busy traffic and movement of heavy and light vehicles. It is observed during summer that predominant wind direction, i.e., southwest (Fig. 2), raised the dust burden at Loc. 3 and Loc. 4. Loc. 4 with a moderately higher value

of dust ($21.34 \pm 5.50 \text{ ton km}^{-2} \text{ month}^{-1}$) is a lawn of a residence (outside the IIT Kharagpur campus) situated near a main road connecting to national highways. The dust load at Loc. 3(traffic area outside the campus) and Loc. 4 (roadside residential area outside the campus) is mostly comprised of suspended road dust generated due to the continuous movement of heavy vehicles. Loc. 1 and Loc. 2 are situated within the campus area and exhibit relatively lower values of dustfall (2.44 ± 0.83 and $6.69 \pm 1.73 \text{ ton km}^{-2} \text{ month}^{-1}$) in March. The dust deposit measured for Loc. 1, a residential area covered with faculty quarters, is found lowest as compared with other three locations in Kharagpur Town. A two-way ANOVA confirmed a significant variation (at $p < 0.05$) between sites and month interactions.

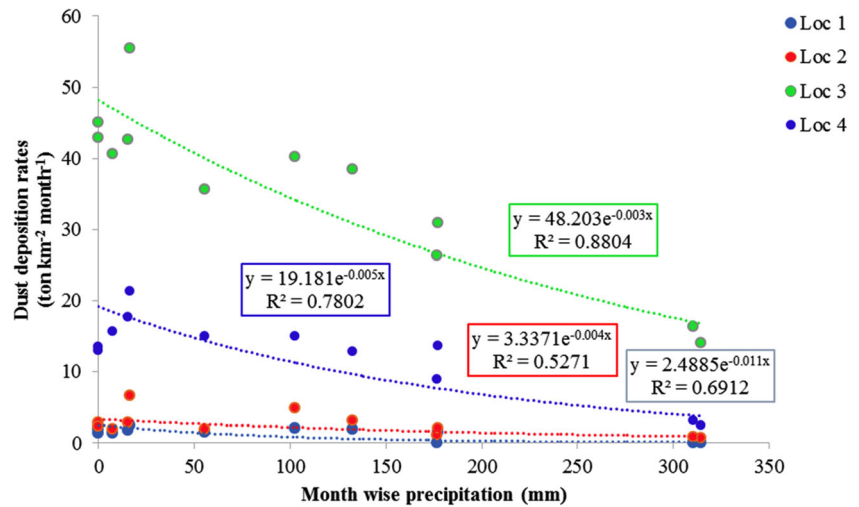
Effect of precipitation on dustfall and its comparison with other studies

Figure 4 shows the effect of rainfall on deposition at different study sites. An exponential regression exhibited a moderate (for Loc. 1 and Loc. 2) to strong (Loc. 3 and Loc. 4) inverse correlation between dust deposition and rainfall ($y = 2.4885E^{-0.011x}$, $R^2 = -0.69$ at Loc. 1; $y = 3.337E^{-0.004x}$, $R^2 = -0.52$ at Loc. 2; $y = 48.20E^{-0.003x}$, $R^2 = -0.88$ at Loc. 3; and $y = 19.18E^{-0.05x}$, $R^2 = -0.78$ at Loc. 4). However, there was no relation found between temperature and dustfall. Table 2 represents a comparison of the dustfall concentration of the present study with other studies conducted in urban areas of some cities. The highest dustfall of $96.2 \text{ ton km}^{-2} \text{ month}^{-1}$ was reported in a study

Table 1 Two-way ANOVA results for mean dustfall deposition rate at different seasons and locations ($*p < 0.05$)

Source	Sum of squares	Degrees of freedom	Mean square	F	Sig.
Location	2.952	3	0.984	63.593	0.000*
Season	0.445	2	0.223	14.393	0.000*
Location* and season	0.392	6	0.065	4.225	0.003*
Error	0.495	32	0.015		
Total	6.472	44			

Fig. 4 Regression plot of dust deposition rate of four study locations with precipitation showing exponential trend



conducted by Pandey et al. (2008) in opencast coalmine area, Bina of India, whereas the lowest average dustfall of $0.83 \text{ ton km}^{-2} \text{ month}^{-1}$ was obtained by Reheis and Kihl (1995) in Southern Nevada (USA). The dustfall study

conducted in Shuwaikh City (Kuwait) showed second highest level of deposition of $53.7 \text{ ton km}^{-2} \text{ month}^{-1}$ (Al-Harbi 2015). In a study conducted in Gansu Province (China), the dustfall rate in the desert and Gobi area and loess area was assessed and

Table 2 Comparison of dustfall concentration of Kharagpur Town with other cities in the world

Study area	Characteristics and sources	Sampling condition	Dustfall deposition rate ($\text{ton km}^{-2} \text{ month}^{-1}$)	Reference
Bina, India	Residential and industrial, opencast coalmines	Monthly sampling for 2 years (June 2002–May 2004)	96.2	Pandey et al. 2008
Shuwaikh City, Kuwait	Partly industrial and partly rural area	Monthly sampling for 1 year (2009)	53.7	Al-Harbi 2015
N-NW of India	Sampling locations were situated between Thar Desert in west and Ganga alluvial plains in eastern part. Hot arid to semiarid climate	Sampling during summer (April–June) and winter (October–February) seasons	21	Yadav and Rajamani 2006
Lanzhou, China	Western loess plateau influenced by dust storm and haze events	2-h interval successive dustfall measurements during typical dust storm and haze events in March and April 1999, together with monthly dust deposition data that extended over a 2-year period, from May 1998 through April 2000	11.08	Liu et al. 2004
Southern Nevada, USA	Covered by southern Great Basin and Mojave Desert	Annual sampling for 5 years from 1984 to 1989 from 55 sites	0.83	Reheis and Kihl 1995
Nagev, Israel	Desert	A decade 1988–1997 study based on 24-h measuring interval	17	Offer and Goossen 2001
Yazd, Iran	Industrial area influenced by sandstorm	Four months sampling from August 2005 to March 2006	6.48	Naddafi et al. 2006
Texas, USA		Sampling done quarterly	8.5	Crabtree 2005
California, USA			1.605	
Arizona, USA			4	
Kharagpur, India	Urban area	One year sampling (June 2014 to June 2015)	13.09	Present study

found in the range of 18.23–69.4 ton km⁻² month⁻¹ and 9.7–34.84 ton km⁻² month⁻¹, respectively (Ta et al. 2004). The dustfall of Kharagpur Town was found to be lowest (13.09 ton km⁻² month⁻¹) among Indian cities. An intermediate value of 21 ton km⁻² month⁻¹ of dustfall was estimated in North and Northwest India by Yadav and Rajamani (2006). There are results of dustfall reported by other studies that are also shown in Table 2 and a significant difference found in dustfall levels among different studies, and this variation could be due to difference in their geographical locations, traffic compositions, and type of industries running over the area.

Trace element concentration in dustfall samples

The descriptive statistics for the twelve samples analyzed for each metal are presented in Table 3. The heterogeneous nature of the dustfall samples gives large SD values shown in the table. The mean values are observed to be higher than upper continental crust (UCC) values except for Sc and Hf. Zr exhibits the highest mean concentration of 209.94 µg/g. The mean values of all trace elements (except Y and Hf) are found greater than background soil values. The high values of skewness, kurtosis, SD, and strong coefficients of variations in the data specify the occurrence of geochemical abnormalities and human activities (Lu et al. 2012).

The coefficients of variance (CVs) of Cr and Pb are higher than 50% as compared with other metals. Skewness of Cr, Ni, and Pb exceeds unity which denotes asymmetry and positively skewed towards lower concentration. Therefore, the data are log-transformed to fulfill the normality assumptions for further statistical analysis. The concentration of trace elements present in dustfall and their comparison with other cities are shown in Table 4. It is observed that there is a considerable variation among the concentrations of trace metals studied in different cities in the world. This variation could be due to

different human activities, land use pattern, and the discrepancy in sampling procedures and digestion methods used for extraction of metals (Joshi et al. 2009).

Metal pollution assessment in dustfall: geoaccumulation index and enrichment factor

The spatial variation of metal pollution (I_{geo} and EF) is observed among the four different locations of Kharagpur Town showing the influence of different land use patterns and anthropogenic activities. The box plot of site-specific I_{geo} and EF for trace elements is shown in Figs. 5 and 6. With respect to Sc, Zr, and Hf, the dustfall samples show practically uncontaminated status with mean $I_{geo} < 0$, while V and Co also exhibit uncontaminated status for Loc. 1 (residential area inside the college campus). The I_{geo} values of elements Cr and Pb from all locations reveal their moderately to heavily contaminated condition, showing an extension of metal pollution in Kharagpur Town. The mean I_{geo} values for Cr show moderately contaminated status for Loc. 1, Loc. 2, and Loc. 3 while Zn shows the same status for Loc. 3 and Loc. 4 also. With respect to Loc. 1 (residential area), most of the elements like Sc, V, Co, Ni, Y, Zr, Ce, and Hf show deficiency to minimal enrichment (EF < 2), while Pb exhibits moderate enrichment with a mean value of 4.50. The dustfall samples collected from Loc. 2 (main gate of IIT Kharagpur campus, traffic site) and Loc. 3 (traffic site near to petrol station) display moderate to significant enrichment for Cr, Co, Ni, Zn, and Pb. The highest mean EFs of 6.70 and 7.18 are observed for Cr and Pb in the dustfall samples of Loc. 4 (residential area near to main road), showing the presence of a significant level of enrichment for these metals. The EF > 15 obtained for Pb derived from dustfall sample of Loc. 2 indicates the contribution of anthropogenic sources.

The average values of I_{geo} of heavy metals in dustfall samples of Kharagpur Town are presented in Fig. 7a. The mean I_{geo}

Table 3 Descriptive statistics of trace element concentration (µg g⁻¹) in dustfall samples collected from Kharagpur Town

Element	Min	Max	Range	Mean	SD	Skewness	Kurtosis	CV (%)	Background soil value	UCC ^a
Sc	5.649	15.808	10.159	11.734	3.180	-0.701	-0.473	27.1	10.43	11
V	51.530	161.371	109.841	115.078	30.435	-0.767	0.640	26.4	50.20	60
Cr	119.769	427.136	307.367	200.454	105.386	1.920	2.328	52.6	3.92	35
Co	8.835	29.119	20.283	22.422	5.873	-1.142	1.278	26.2	0.26	10
Ni	28.210	111.101	82.891	55.966	21.980	1.689	3.139	39.3	3.23	20
Zn	120.232	322.973	202.741	219.968	50.936	0.038	1.263	23.2	26.08	71
Y	10.215	48.238	38.023	31.558	13.288	-0.085	-1.481	42.1	38.90	22
Zr	94.474	325.597	231.123	209.941	63.134	-0.107	0.420	30.1	83.80	190
Ce	38.683	142.310	103.627	99.695	36.287	-0.834	-0.752	36.4	86.50	64
Hf	2.301	6.806	4.505	4.778	1.338	-0.508	-0.427	28.0	4.70	5.8
Pb	64.735	891.522	826.786	194.876	226.524	3.109	10.110	116.0	0.98	20

^a UCC upper continental crust proposed by Taylor and McLennan (1985)

Table 4 Comparison of atmospheric deposition of trace elements between the Kharagpur Town and other cities of the world

Area	Characteristic	Zn	Cr	Co	Pb	Ni	V	Zr	Ce	Y	Hf	Sc	Digestion procedure	Sampling method	Reference
Elazığ, Turkey	Industrial	–	364.75	160.1	1635.95	544	–	–	–	–	–	–	–	Dustfall collectors	Arslan and Boybay 1990
Zarqa, Jordan	Industrial	639.8	65.5	–	59.5	–	–	–	–	–	–	–	HNO ₃	Polyethylene dustfall containers	Jaradat et al. 2004
Raipur, Central India	Urban	3.79	0.234	–	–	0.211	–	–	–	–	–	–	HNO ₃	Glass jars	Thakur et al. 2004
Yangtze River Delta, East China	Industrial and commercial	696	119.8	–	–	–	–	–	–	–	–	–	HCl+HNO ₃ +HF+HClO ₄	Porcelain cylindrical jar	Huang et al. 2009
Asyut, Egypt	Industrial	235.00	–	–	22.33	–	–	–	–	–	–	–	HNO ₃	Dustfall collectors	Mohamed et al. 2013
Jharia, India	Commercial and residential sites near coal mining area	253	47.95	16.25	58.7	35.6	51.45	–	–	–	–	–	HNO ₃ +HClO ₄ +H ₂ SO ₄	Dustfall jar	Rout et al. 2014
North China	Industrial	614.8	125.6	16.1	154.0	56.9	82.4	146.3	62.3	22.2	3.3	8.3	HNO ₃ +HF+HClO ₄	Plastic jars	Xiong et al. 2015
Kharagpur, India	Urban	219.96	200.45	22.42	194.87	56	115.08	209.94	99.69	31.55	4.77	11.73	HNO ₃ +HF+HClO ₄	Dustfall jar	Present study

values for Zn and Cr are 1.08 and 1.6, respectively. These values belong to class 2 of the descriptive classification of Muller 1981 indicating moderate concentration. The mean I_{geo} values of Sc, V, Co, Ni, Y, Zn, Ce, and Hf exhibit uncontaminated to moderately uncontaminated status. The average I_{geo} value of lead at 2.01 indicates moderately to heavily contaminated category. Around 42% I_{geo} value of Pb belongs to the class between 3 and 4 and 17% of I_{geo} value of lead range between 4 and 5. Therefore, 59% of I_{geo} value for Pb suggests heavily contaminated status.

The values of EFs for the metals in the dustfall samples are presented in Fig. 7b. The average EF values of Sc, V, Y, Zr, Ce, and Hf are below 2 indicating minimal enrichment, whereas the average EF values of Zn, Co, Ni, and Cr are 2.98, 2.21, 2.28, and 4.39, respectively. The latter groups of metals are therefore moderately enriched. As in the case of I_{geo} values, lead exhibits wide variability in the enrichment factors. The range of EF value for Pb is from 3.03 to 41.79 with a mean of 5.68. Around 58% of Pb samples belong to the class of significant enrichment, and 8.33% of Pb samples belong to very high to extremely high enrichment class.

The values of I_{geo} and EFs for trace elements in the soil sample are also calculated and presented in Fig. (S1) and Fig. (S2). The I_{geo} values of all elements of background soil sample are below unity, showing uncontaminated status. Similarly, the EF values of all elements are also below 2, indicating minimal enrichment of trace elements in the background soil. Therefore, the heavy metals in dustfall samples are found significantly enriched in comparison with the background soil indicating the substantial contribution of anthropogenic sources in Kharagpur Town.

Correlation analysis

Table 5 presents the Pearson rank correlation statistics among the twelve metals examined. A very significant correlation is found between certain metal pairs at 0.01 level of significance. This includes Ni–Cr (0.923), Hf–Sc (0.937), Pb–Ni (0.90), and V–Sc (0.85). The correlation matrix exhibits poor to negative correlation between the other metal sets mainly of Cr, Zn, and Ni individually with Y, V, Ce, Zr, and Hf. The latter group is seen to exhibit minimal enrichment ($EF < 2$) and belong to practically uncontaminated category ($I_{geo} \leq 0$). The anthropogenic activities at Kharagpur Town, therefore, have no contribution towards the creation of these metals, whereas Zn, Cr, Ni, and Pb come from automobile parts and accumulated in the road dust by vehicular and fugitive emissions. Additionally, some other activities like domestic operations and natural sources are also considered as secondary sources to generate those metals. This is supported by the fact that two of the sampling locations, Loc. 3 (petrol station) and Loc. 4 (roadside residential area), are in the influence of heavy traffic movement and the vicinity of road side of automobile repair and service outlets.

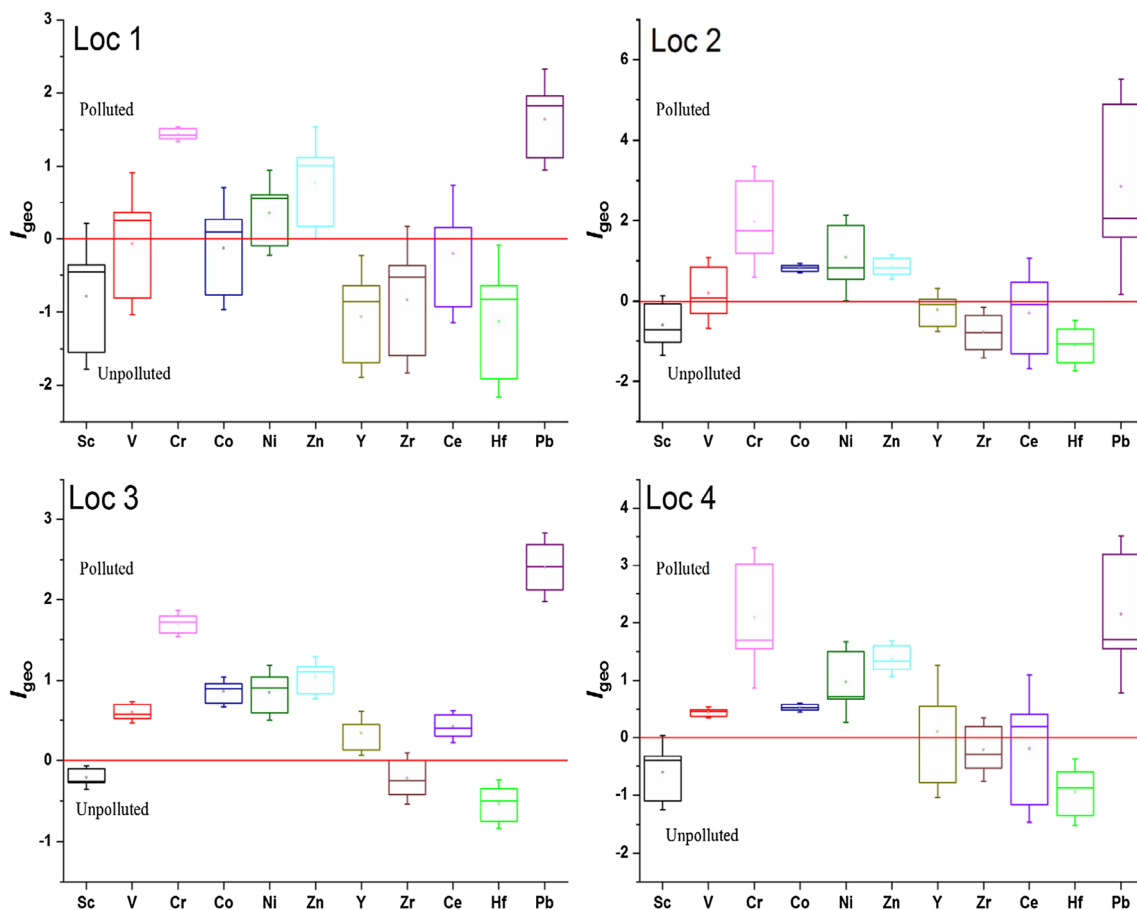


Fig. 5 Box plot of I_{geo} of heavy metals in dustfall samples from four locations of Kharagpur Town

Principal component analysis

PCA is applied to determine the possible contributing factors towards metal concentration and to identify their common origin in the dustfall samples. Table 6 presents the results of percentage of variance and factor loadings based on varimax rotation. For varimax rotation, the number of significant principal components with eigenvalue more than or equal to one is selected. All the metals are well represented by the four factors, and the factor loadings greater than 0.5 (italicized in Table 6) are regarded as significant for interpretation of the data. Table 6 presents the four principal components contributing 95% of the total variance. Out of these, 26.6% is controlled by factor 1 having initial eigenvalues 4.98 showing higher loading for Cr, Ni, and Pb, while the loadings of Co are more than 0.5 but less as compared with loadings of the other metals in this group. From the total variance calculated, 26% is explained by factor 2 (shown in Table 6). High factor loadings are noted for Sc (0.861), Hf (0.805), Y (0.772), Co (0.707), and V (0.623) (Table 6). The dominant metals of factor 1 category (Cr, Ni, Co, and Pb) are seen to have negative correlation as per Table 5 when compared with the dominant metals of factor 2 category (Sc, Y, V, Co, and Hf). These findings reinforce the distinct nature of sources of origin

between these two groups of metals. Although the loading of V (0.734) is lower than other metals in the group, the rotated component matrix shows that V shows a joint relationship with factor 2 and factor 3 suggesting that it has a combined origin. Table 6 shows that V exhibits strong correlation with Ce, Hf, and Co but low to negative correlation with Zn, Cr, and Ni. The factor loadings from Table 6 point out that V (0.623), Co (0.582, 0.707), and Y (0.772, 0.578) have multiple sources of origin. This factor explains mixed sources with contribution from industrial processes like metal processing as well as vehicular and domestic activity (Mathur et al. 2016). The presence of small-scale industries like metal processing or sponge iron plant (TATA Metaliks), thermal power plant (Bengal Energy Ltd.), and vehicular traffic and domestic activity might be the possible mixed sources for generation of heavy metals in Kharagpur Town.

Factor 4 is dominated by Zn and Y explaining 17.6% of total variance. In the present study, Zn exhibits positive correlation with Y (0.56) and absolutely no correlation with any other elements. Additionally, Zn exhibits high mean level concentration in comparison with their corresponding crustal abundances (Table 6), indicating its specific origin. Zn is used in the manufacturing of automobile parts like tire, brake, and the brake lining systems and emitted to the surface dust due to

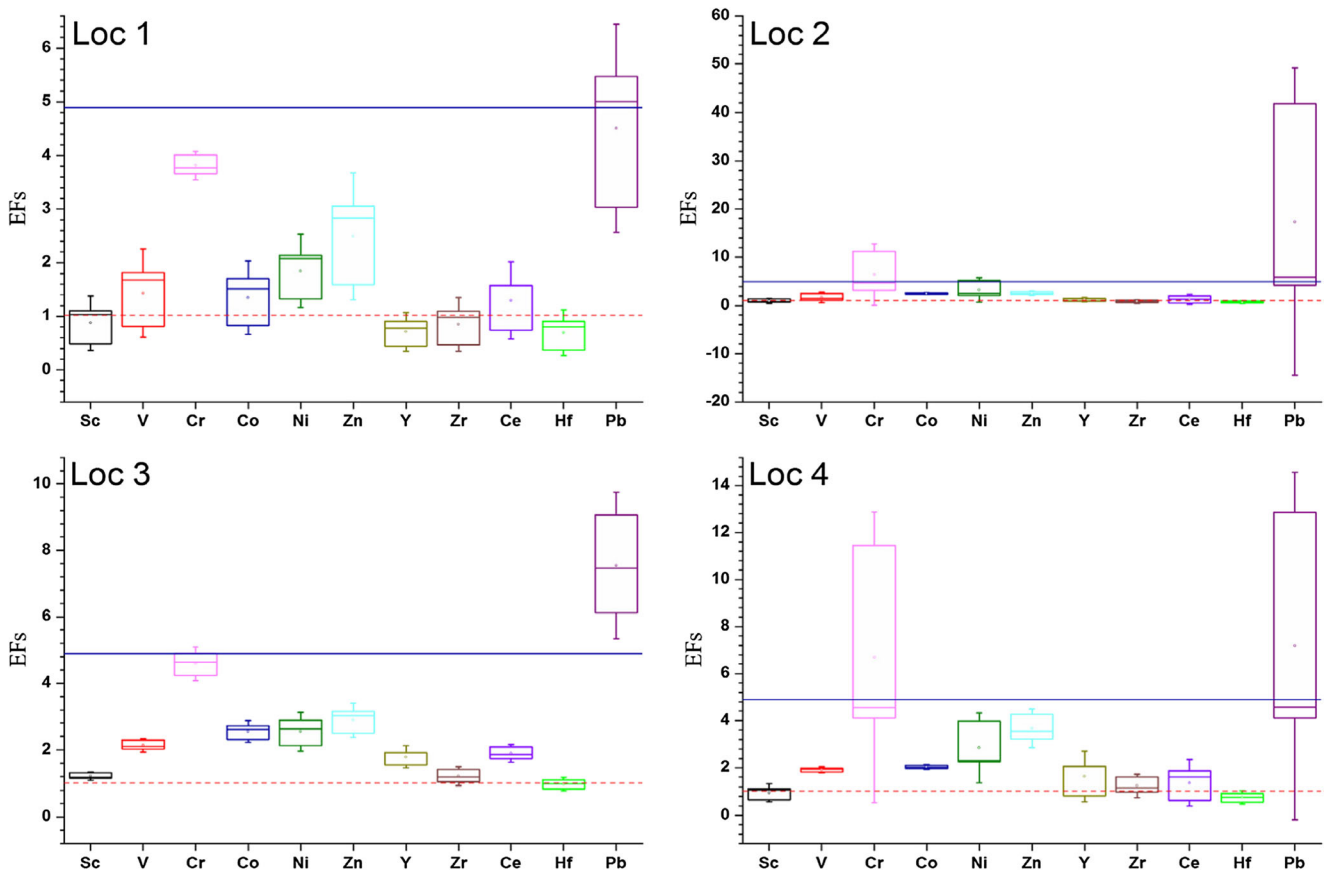


Fig. 6 Box plot of EFs of heavy metals in dustfall samples from four locations of Kharagpur Town

nonexhaust emissions by mechanical abrasion of automobile parts (Mathur et al. 2016) and abrasion of tire tread against road surface. Therefore, tire dust is reported as one of the sources of Zn in the urban environment (Adachi and Tainosho 2004).

Health risk assessment of heavy metal exposure from dustfall in Kharagpur

Table 7 illustrates the results of health risk assessment of metals including hazard quotient for the three pathways (ingestion, inhalation, and dermal) and the hazard index for each of the metals in the dustfall of Kharagpur Town. The reference doses for noncarcinogenic effects due to oral and dermal pathways are available for five of the metals examined. These are Cr, Co, Zn, Pb, and Ni. The inhalation risk is determined for Cr and Co because reference doses for inhalation pathway are available for only those two metals (Lu et al. 2014).

The ingestion pathway has a higher noncarcinogenic risk in comparison with the dermal pathway for all the metals studied. The inhalation risk is determined for Cr and Co only. In the case of Co, the inhalation HQ_{inh} is in between HQ_{ing} and HQ_{dermal} , while in the case of Cr, HQ_{inh} is a least out of the three pathways. HQ_{inh} is calculated for the Cr and Co due to the availability of RfD (inhalation). In the calculation of HI for the other metals, HQ_{inh} values are taken as zero. It can be seen that as such the

HQ_{inh} values are lower to HQ_{ing} by order of two. Therefore, the omission becomes justifiable. HI is essentially dominated by HQ_{ing} and out of the HI values computed; Pb emerges as a metal of the highest noncarcinogenic risk for adults which are also true for children. The noncarcinogenic risk as determined by HI decreases in the order of $Pb > Cr > Co > Ni > Zn$ both for adults and children. When we examine the relative risk of children on adults for the different metals, Co has the highest ratio at 9.36 while Cr has the lowest ratio at 3.53. Carcinogenic risk assessment for adults as well as children is carried out for Cr, Co, and Ni only, and the inhalation exposure mode is considered in the model. Calculated risk values are shown in Table 7. The results show that the cancer risk of Cr, Co, and Ni estimated for adults and children is lower than the acceptable range (10^{-6} to 10^{-4}).

Discussion

The contamination assessment was carried out using the geoaccumulation index and enrichment factor procedures. By I_{geo} , Zn (1.08) and Cr (1.6) are seen to represent moderate contamination. Lead exhibited slightly higher I_{geo} (2.01) suggesting higher level of contamination when compared with the other three metals. Sc, V, Co, Ni, Y, Zr, Ce, and Hf have I_{geo} values less than one, suggesting practically uncontaminated status. The

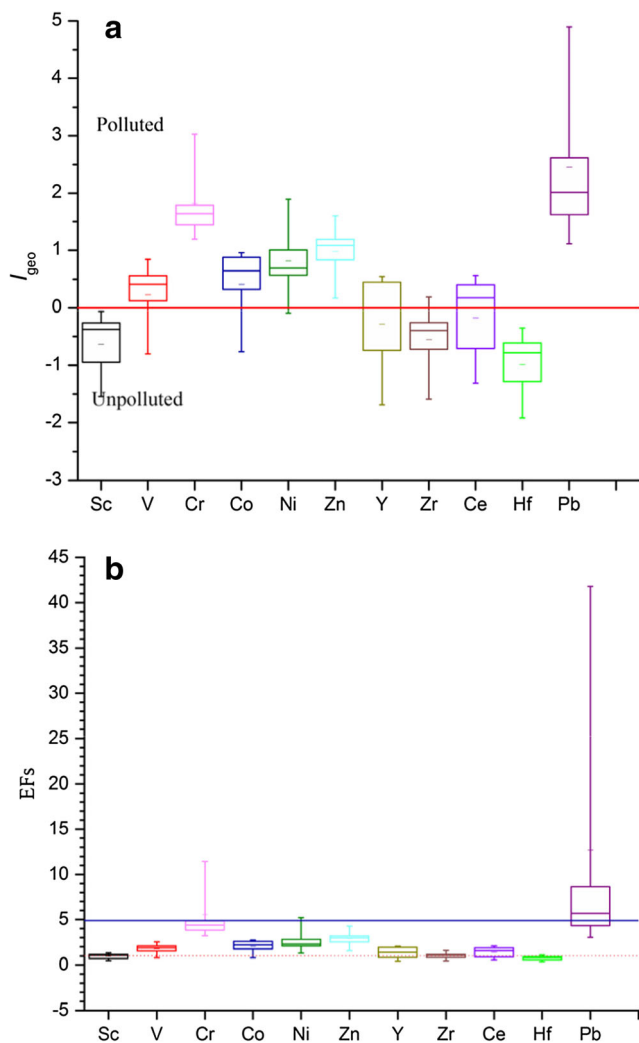


Fig. 7 Box plot of **a** I_{geo} and **b** EF for heavy metals in dustfall samples of Kharagpur

Table 6 Rotated component matrix of trace elements studied for Kharagpur Town

Metal	Component			
	1	2	3	4
Sc	-0.244	<i>0.861</i>	0.379	-0.094
V	-0.045	<i>0.623</i>	<i>0.734</i>	0.069
Cr	<i>0.913</i>	-0.334	0.145	0.098
Co	<i>0.582</i>	<i>0.707</i>	0.247	-0.001
Ni	<i>0.991</i>	-0.023	0.036	-0.005
Zn	-0.111	0.018	-0.170	<i>0.964</i>
Y	-0.110	<i>0.772</i>	0.006	<i>0.578</i>
Zr	0.126	0.215	<i>0.896</i>	0.277
Ce	-0.131	0.304	<i>0.851</i>	-0.206
Hf	-0.260	<i>0.805</i>	0.419	0.015
Pb	<i>0.915</i>	-0.054	-0.334	-0.158
Eigenvalue	4.984	3.099	1.983	1.218
% of variance	26.625	26.077	23.720	17.617
Cumulative %	26.625	52.702	76.422	94.038

Factor loadings > 0.5 are shown as italicized characters

enrichment factor values point out that Sc, V, Y, Zr, Ce, and Hf are minimally enriched while Zn, Co, Ni, and Cr are moderately enriched. Cr presented the highest enrichment factor at 4.39 followed by Zn, Ni, and Co. The order of decrease for the enrichment factors is Cr (4.39) > Zn (2.99) > Ni (2.28) > Co (2.21). The Co with minimum enrichment factor as compared with other elements ensures its sources from resuspended soil dust and fossil fuel combustion (Al-Momani 2003; Schleicher et al. 2011). Some anthropogenic sources such as diesel and fossil fuel combustion and automotive emissions are also reported as a source of Ni pollution in the atmosphere (Manoli et al. 2002; Wang et al. 2003; Duong and Lee 2011; Al-Khashman 2013).

Table 5 Pearson’s correlation matrix of heavy metals in the dustfall samples of Kharagpur Town

	Sc	V	Cr	Co	Ni	Zn	Y	Zr	Ce	Hf	Pb
Sc	1										
V	0.852 ^b	1									
Cr	-0.448	-0.109	1								
Co	0.510	0.577	0.299	1							
Ni	-0.235	-0.032	0.923 ^b	0.544	1						
Zn	-0.100	-0.022	-0.026	-0.116	-0.115	1					
Y	0.608 ^a	0.514	-0.299	0.499	-0.133	0.569	1				
Zr	0.475	0.800 ^b	0.215	0.411	0.157	0.114	0.299	1			
Ce	0.589 ^a	0.768 ^b	-0.142	0.401	-0.115	-0.331	0.195	0.696 ^a	1		
Hf	0.937 ^b	0.793 ^b	-0.439	0.458	-0.242	-0.004	0.619 ^a	0.582 ^a	0.566	1	
Pb	-0.369	-0.344	0.788 ^b	0.386	0.900 ^b	-0.192	-0.248	-0.232	-0.391	-0.393	1

^a Correlation is significant at the 0.05 level (two-tailed)

^b Correlation is significant at the 0.01 level (two-tailed)

Table 7 Hazard quotient, hazard indices, and cancer risk of different exposure pathways for metals

	Cr (noncanc.)	Cr (canc)	Co (noncanc.)	Co (canc)	Zn	Pb	Ni (noncanc.)	Ni (canc)
C (95% UCL)	268.63		24.61		244.37	365.53	69.74	
Oral R _f D	3.00E-03		3.00-04		3.00E-01	3.50E-03	2.00E-02	
Dermal R _f D	6.00E-05		1.60E-02		6.00E-02	5.25E-04	5.00E-03	
Inhal. R _f D	2.86E-05		5.71E-06		NA	NA	NA	
BAF	0.058		0.045		0.532	0.372	0.324	
Inhal. SF		4.20E+01		9.80E+00				8.40E+01
Adults								
HQ _{ing}	7.46E-03		5.27E-03		6.19E-04	5.55E-02	1.61E-03	
HQ _{inh}	1.15E-04		4.08E-05		AN	AN	AN	
HQ _{dermal}	1.49E-02		3.95E-06		1.24E-04	1.48E-02	2.39E-04	
HI = ΣHQ _i	2.25E-02		5.32E-03		7.43E-04	7.03E-02	1.85E-03	
Risk		4.74E-08		7.82E-10				1.37E-09
Children								
HQ _{ing}	6.96E-02		4.92E-02		5.78E-03	5.18E-01	1.51E-02	
HQ _{inh}	2.04E-04		7.23E-05		AN	AN	AN	
HQ _{dermal}	9.74E-03		2.58E-06		8.09E-05	9.67E-03	1.56E-04	
HI = ΣHQ _i	7.96E-02		4.93E-02		5.86E-03	5.28E-01	1.52E-02	
HI _{children} /HI _{adults}	3.53		9.26		7.89	7.51	8.2	
Risk		2.1E-08		3.47E-10				6.06E-10

NA not available, AN assumed negligible (Kurt-Karakus 2012)

The high enriched Cr, compared with other mentioned elements (Zn, Ni, and Co), seems to originate from man-made activities like biomass burning and vehicle emissions (Salvador et al. 2004; Norouzi et al. 2017). These are metals belong to the moderately enriched category based on the Sutherland (2000) classification. The Pearson correlation statistics revealed the existence of significant correlation between certain metal pairs at 0.01 level of significance. These include Ni–Cr ($r = 0.923$), Hf–Sc ($r = 0.937$), Pb–Ni ($r = 0.9$), and V–Sc ($r = 0.85$). Multivariate factor analysis (PCA) was applied to the sample data to identify the common origin in the dustfall samples. The results show that four principal components contribute to 95% of the total variance. The factor 1 group with Cr, Ni, and Pb shows higher loading. The dominant metals in the factor 2 group having higher loadings are Sc, Hf, Y, Co, and V. The negative correlation between dominant metals of factor 1 and the dominant metals of factor 2 indicates the distinct nature of the sources of origin of these two groups of metals. The high factor loadings observed for V (0.623), Co (0.582, 0.707), and Y (0.772, 0.578) point out the multiple sources of origin of these metals. The dominated metals of the factor 3 group are V, Zr, and Ce while the corresponding metals for the factor 4 groups are Zn and Y. The result of PCA in combination with enrichment factor values indicated that Sc, V, Co, Y, Zr, Ce, and Hf have natural sources of origin, whereas Cr, Ni, Zn, and Pb have anthropogenic sources of origin, attributed to tailpipe emission, tyre wear and corrosion of automobile parts, emission from metal working, sponge iron plant, and manufacturing unit located in Kharagpur Town.

In the present study, soil sample analysis shows significantly low concentration of almost all trace elements compared with dustfall samples except for Y. Additionally, Cr, Co, Ni, Zn, and Pb were found negligible in background soil as compared with dustfall. However, the content of Y, V, Sc, Ce, and Hf were found minimal enrichment in the dustfall, but these elements (Y, V, Sc, Ce, and Hf) were detected in background soil with considerable concentration. These findings confirm that the metals (Cr, Co, Ni, Zn, and Pb) with significant concentration in dustfall would have originated from traffic-related sources, and the presence of other groups of elements (Y, V, Sc, Ce, and Hf) could be attributed to crustal origin.

The hazard quotient and hazard index parameters were determined for five of the heavy metals (for which R_fD values are available in the literature) using the risk assessment model developed by US EPA (1996). The noncancer risk on health represented by hazard index is seen to decrease in the order of Pb > Cr > Co > Ni > Zn both for children and adults. The HI values are less than unity for the Kharagpur Town, for the five metals suggesting that there is no significant noncancer risk from these metals. Pb exhibits the highest HI for children at a value of 0.528. The study did not identify any metal with HI greater than one for the Kharagpur Town. Only HI for Pb comes closer to one for children who may be naturally exhibited higher risk in comparison with adults such that the ratio between HI for children and HI for adults varies from 3.53 to 9.26 for the metals investigated. The carcinogenic risk estimated for adults and children shows values lower than

acceptable range. Although the results of risk assessment presented in this work are valid, but several uncertainty factors are also involved. One important source of uncertainty is due to the lack of bioaccessibility data (Turner 2011). Apart from that, a significant uncertainty arises for using the default values assigned to the several exposure variables such as dermal absorption factors (ABS) (Barrio-Parra et al. 2018).

Conclusions

In this study, the seasonal variation in dustfall concentration, as well as its chemical constituents, has been thoroughly investigated for 1 year in four study locations of Kharagpur Town, India, for the first time. Among the four representative sampling locations, two are residential and traffic area inside the IIT Kharagpur campus, whereas the other two are residential and traffic area situated outside the campus. The representative dustfall samples were collected and studied in the laboratory. It is concluded from the findings that ambient level dustfall deposition is higher during summer months over the whole area. The high deposition might be due to high temperature and low humidity, and calm conditions occur during this season. ANOVA results also agreed that there is a significant seasonal variation in the concentration of dustfall over the months ($p < 0.05$). Out of four study locations, the highest dustfall deposition is recorded in the outside campus traffic area where a petrol filling station is located, whereas the lowest value occurred in the residential area inside the campus. Occurrence of higher degree of spatial variability across all study locations is probably due to variation in the source characteristics with potential effect of local sources on dustfall generation. Overall, the pollution load at the IIT Kharagpur campus is less compared with the area outside the campus, due to less traffic density and extensive vegetation cover. This study further analyzes the elemental composition and finds that dustfall from Kharagpur Town is enriched with some metals like Zn, Cr, Ni, and Co and is contributed by vehicle activities like vehicle exhaust emissions, mechanical abrasion, and corrosions of metallic automobile body parts. Dust-bound trace elements are found with high level of contamination of Pb and moderate contamination for Zn and Cr. The calculated results of EF reveal the significant enrichment of Pb and moderate enrichment of Zn, Co, Ni, and Cr. Heavy metals considered in this study are unlikely to pose carcinogenic risk for adults and children based on inhalation exposure pathway. The presence of these metals also indicates that there must be some contribution by small-scale industries named TATA Metaliks and Bengal Energy present in Kharagpur Town. The present study concludes that the human health risk associated with heavy metals is within the permissible limit at the town. However, Kharagpur is a growing town with several small and large-scale industries, dense traffic, and population, which might

contribute to the pollution load in the future. Hence, a regular assessment of air quality and human health risk is very much required, and our study could be considered as a baseline study.

Acknowledgments The authors are thankful to the director, CSIR-National Geophysical Research Institute, Hyderabad, for providing the technical support in analyzing the samples using HR-ICP-MS.

Compliance with ethical standards

Conflict of interest The authors declare that they have no conflict of interest.

References

- Adachi K, Tainosho Y (2004) Characterization of heavy metal particles embedded in tire dust. *Environ Int* 30:1009–1017. <https://doi.org/10.1016/j.envint.2004.04.004>
- Adachi K, Tainosho Y (2005) Single particle characterization of size-fractionated road sediments. *Appl Geochem* 20:849–859. <https://doi.org/10.1016/j.apgeochem.2005.01.005>
- Adamiec E, Jarosz-Krzemińska E, Wieszała R (2016) Heavy metals from non-exhaust vehicle emissions in urban and motorway road dusts. *Environ Monit Assess* 188:1–11. <https://doi.org/10.1007/s10661-016-5377-1>
- Al-Harbi M (2015) Characteristics and composition of the falling dust in urban environment. *Int J Environ Sci Technol* 12:641–652. <https://doi.org/10.1007/s13762-013-0440-8>
- Al-Khashman OA (2007) Determination of metal accumulation in deposited street dusts in Amman. *Jordan Environ Geochem Health* 29:1–10. <https://doi.org/10.1007/s10653-006-9067-8>
- Al-Khashman OA (2013) Assessment of heavy metals contamination in deposited street dusts in different urbanized areas in the city of Ma'an, Jordan. *Environ Earth Sci* 70:2603–2612. <https://doi.org/10.1007/s12665-013-2310-6>
- Al-Momani IF (2003) Trace elements in atmospheric precipitation at Northern Jordan measured by ICP-MS: acidity and possible sources. *Atmos Environ* 37:4507–4515. [https://doi.org/10.1016/S1352-2310\(03\)00562-4](https://doi.org/10.1016/S1352-2310(03)00562-4)
- Apeaygei E, Bank MS, Spengler JD (2011) Distribution of heavy metals in road dust along an urban-rural gradient in Massachusetts. *Atmos Environ* 45:2310–2323. <https://doi.org/10.1016/j.atmosenv.2010.11.015>
- Arslan M, Boybay MA (1990) Study on the characterization of dustfall. *Atmos Environ A Gen* 24:2667–2671. [https://doi.org/10.1016/0960-1686\(90\)90146-E](https://doi.org/10.1016/0960-1686(90)90146-E)
- ASTM (2004) Standard test method for collection and measurement of dustfall (settleable particulate matter). American Society for Testing and Materials—ASTM D1739/ 98
- Atiemo MS, Ofosu GF, Kuranchie-Mensah H, Tutu AO, Palm ND, Blankson SA (2011) Contamination assessment of heavy metals in road dust from selected roads in Accra, Ghana. *Res J Environ Earth Sci* 3:473–480
- Balakrishna G, Pervez S (2009) Source apportionment of atmospheric dust fallout in an urban-industrial environment in India. *Aerosol Air Qual Res* 9:359–367. <https://doi.org/10.4209/aaqr.2008.12.0065>
- Banerjee ADK (2003) Heavy metal levels and solid phase speciation in street dusts of Delhi India. *Environ Pollut* 123:95–105. [https://doi.org/10.1016/S0269-7491\(02\)00337-8](https://doi.org/10.1016/S0269-7491(02)00337-8)
- Barrio-Parra F, De Miguel E, Lázaro-Navas S, Gómez A, Izquierdo M (2018) Indoor dust metal loadings: a human health risk assessment. *Expo Health* 10:41–50. <https://doi.org/10.1007/s12403-017-0244-z>

- Buat-Menard P, Chesselet R (1979) Variable influence of the atmospheric flux on the trace metal chemistry of oceanic suspended matter. *Earth Planet Sci Lett* 42:399–411. [https://doi.org/10.1016/0012-821X\(79\)90049-9](https://doi.org/10.1016/0012-821X(79)90049-9)
- Chate DM, Pranesha TS (2004) Field studies of scavenging of aerosols by rain events. *J Aerosol Sci* 35:695–706. <https://doi.org/10.1016/j.jaerosci.2003.09.007>
- Church TM, Scudlark JR (1998) Trace metals in estuaries: a Delaware Bay synthesis. In: Allen HE, Garrison AW, Luther III GW (ed) *Metal speciation and contamination of surface water*, 3rd edn. Ann Arbor Press, Inc, Chelsea, pp. 1–21
- Crabtree GW (2005) Dust fall on the southern high plains of Texas. Dissertation, Texas Tech University
- Dasgupta T (1983) Investigation for lays in the Midnapore district, West Bengal. Geological survey of India. <https://employee.gsi.gov.in/cs/groups/public/documents/document/b3zp/mtix/~edispl/dcpport1gsigovil21729.pdf>. Accessed 26
- Duong TT, Lee BK (2011) Determining contamination level of heavy metals in road dust from busy traffic areas with different characteristics. *J Environ Manag* 92:554–562. <https://doi.org/10.1016/j.jenvman.2010.09.010>
- Faiz Y, Tufail M, Javed MT, Chaudhry MM (2009) Road dust pollution of Cd, Cu, Ni, Pb and Zn along Islamabad Expressway, Pakistan. *Microchem J* 92:186–192. <https://doi.org/10.1016/j.microc.2009.03.009>
- Ferreira-Baptista L, De Miguel E (2005) Geochemistry and risk assessment of street dust in Luanda, Angola: a tropical urban environment. *Atmos Environ* 39:4501–45312. <https://doi.org/10.1016/j.atmosenv.2005.03.026>
- Freiman MT, Hirshel N, Broday DM (2006) Urban-scale variability of ambient particulate matter attributes. *Atmos Environ* 40:5670–5684. <https://doi.org/10.1016/j.atmosenv.2006.04.060>
- Ghosh S, Guchhait SK (2015) Characterization and evolution of laterites in West Bengal: implication on the geology of Northwest Bengal Basin. *Transactions* 37:93–119
- Gope M, Masto RE, George J, Hoque RR, Balachandran S (2017) Bioavailability and health risk of some potentially toxic elements (Cd, Cu, Pb and Zn) in street dust of Asansol, India. *Ecotoxicol Environ Saf* 138:231–241. <https://doi.org/10.1016/j.ecoenv.2017.01.008>
- Green LC, Armstrong SR (2003) Particulate matter in ambient air and mortality: toxicologic perspectives. *Regul Toxicol Pharmacol* 38:326–335. [https://doi.org/10.1016/S0273-2300\(03\)00099-0](https://doi.org/10.1016/S0273-2300(03)00099-0)
- Guo J, Xu Q, Jing W-H (2006) The changing law and trend of dustfall in Beijing during the recent years. *Environ Monitor China* 22:49–52 (in Chinese)
- Gurugubelli B, Pervez S, Tiwari S (2013) Characterization and spatio-temporal variation of urban ambient dust fallout in Central India. *Aerosol Air Qual Res* 13:83–96. <https://doi.org/10.4209/aaqr.2012.06.0141>
- Han Y, Cao J, Posmentier ES, Fung K, Tian H, An Z (2008) Particulate-associated potentially harmful elements in urban road dusts in Xi'an, China. *Appl Geochem* 23:835–845. <https://doi.org/10.1016/j.apgeochem.2007.09.008>
- Hao J, He D, Wu Y, Fu L, He K (2000) A study of the emission and concentration distribution of vehicular pollutants in the urban area of Beijing. *Atmos Environ* 34:453–465. [https://doi.org/10.1016/S1352-2310\(99\)00324-6](https://doi.org/10.1016/S1352-2310(99)00324-6)
- Holnicki P, Kahuszko A, Nahorski Z, Stankiewicz K, Trapp W (2017) Air quality modeling for Warsaw agglomeration. *Arch Environ Prot* 43:48–64. <https://doi.org/10.1515/aep-2017-0005>
- Hu X, Zhang Y, Luo J, Wang T, Lian H, Ding Z (2011) Bioaccessibility and health risk of arsenic, mercury and other metals in urban street dusts from a mega-city, Nanjing, China. *Environ Pollut* 159:1215–1221. <https://doi.org/10.1016/j.envpol.2011.01.037>
- Huang S, Tu J, Liu H, Hua M, Liao Q, Feng J, Weng Z, Huang G (2009) Multivariate analysis of trace element concentrations in atmospheric deposition in the Yangtze River Delta, East China. *Atmos Environ* 43:5781–5790. <https://doi.org/10.1016/j.atmosenv.2009.07.055>
- Jaradat QM, Momani KA, Jbarah AA, Massadeh A (2004) Inorganic analysis of dust fall and office dust in an industrial area of Jordan. *Environ Res* 96:139–144. <https://doi.org/10.1016/j.envres.2003.12.005>
- Joshi UM, Vijayaraghavan K, Balasubramanian R (2009) Elemental composition of urban street dusts and their dissolution characteristics in various aqueous media. *Chemosphere* 77:526–533. <https://doi.org/10.1016/j.chemosphere.2009.07.043>
- Katz M (1969) *Measurement of air pollutants—guide to selection of methods*. World Health Organization, Geneva
- Khorshid MSH, Thiele-Bruhn S (2016) Contamination status and assessment of urban and non-urban soils in the region of Sulaimani City, Kurdistan, Iraq. *Environ Earth Sci* 75:1171. <https://doi.org/10.1007/s12665-016-5972-z>
- Khuzestani RB, Sourì B (2013) Evaluation of heavy metal contamination hazards in nuisance dust particles, in Kurdistan Province, western Iran. *J Environ Sci* 25:1346–1354. [https://doi.org/10.1016/S1001-0742\(12\)60147-8](https://doi.org/10.1016/S1001-0742(12)60147-8)
- Kong S, Lu B, Ji Y, Zhao X, Bai Z, Xu Y, Liu Y, Jiang H (2012) Risk assessment of heavy metals in road and soil dusts within PM_{2.5}, PM₁₀ and PM₁₀₀ fractions in Dongying City, Shandong Province, China. *J Environ Monit* 14:791–803. <https://doi.org/10.1039/C1EM10555H>
- Kumar S (2013) Appraisal of heavy metal concentration in selected vegetables exposed to different degrees of pollution in Agra, India. *Environ Monit Assess* 185:2683–2690. <https://doi.org/10.1007/s10661-012-2739-1>
- Kurt-Karakus PB (2012) Determination of heavy metals in indoor dust from Istanbul, Turkey: estimation of the health risk. *Environ Int* 50:47–55. <https://doi.org/10.1016/j.envint.2012.09.011>
- Leung AO, Duzgoren-Aydin NS, Cheung KC, Wong MH (2008) Heavy metals concentrations of surface dust from e-waste recycling and its human health implications in Southeast China. *Environ Sci Technol* 42:2674–2680. <https://doi.org/10.1021/es071873x>
- Li X, Poon CS, Liu PS (2001) Heavy metal contamination of urban soils and street dusts in Hong Kong. *Appl Geochem* 16:1361–1368. [https://doi.org/10.1016/S0883-2927\(01\)00045-2](https://doi.org/10.1016/S0883-2927(01)00045-2)
- Li HH, Chen LJ, Yu L, Guo ZB, Shan CQ, Lin JQ, Gu YG, Yang ZB, Yang YX, Shao JR, Zhu XM, Cheng Z (2017) Pollution characteristics and risk assessment of human exposure to oral bioaccessibility of heavy metals via urban street dusts from different functional areas in Chengdu, China. *Sci Total Environ* 586:1076–1084. <https://doi.org/10.1016/j.scitotenv.2017.02.092>
- Liu LY, Shi PJ, Gao SY, Zou XY, Erdon H, Yan P, Li XY, Ta WQ, Wang JH, Zhang CL (2004) Dustfall in China's western loess plateau as influenced by dust storm and haze events. *Atmos Environ* 38:1699–1703. <https://doi.org/10.1016/j.atmosenv.2004.01.003>
- Loska K, Wiechula D, Korus I (2004) Metal contamination of farming soils affected by industry. *Environ Int* 30:159–165. [https://doi.org/10.1016/S0160-4120\(03\)00157-0](https://doi.org/10.1016/S0160-4120(03)00157-0)
- Lu X, Li LY, Wang L, Lei K, Huang J, Zhai Y (2009a) Contamination assessment of mercury and arsenic in roadway dust from Baoji, China. *Atmos Environ* 43:2489–2496. <https://doi.org/10.1016/j.atmosenv.2009.01.048>
- Lu X, Wang L, Lei K, Huang J, Zhai Y (2009b) Contamination assessment of copper, lead, zinc, manganese and nickel in street dust of Baoji, NW China. *J Hazard Mater* 161:1058–1062. <https://doi.org/10.1016/j.jhazmat.2008.04.052>
- Lu X, Wang L, Li LY, Lei K, Huang L, Kang D (2010) Multivariate statistical analysis of heavy metals in street dust of Baoji, NW China. *J Hazard Mater* 173:744–749. <https://doi.org/10.1016/j.jhazmat.2009.09.001>

- Lu A, Wang J, Qin X, Wang K, Han P, Zhang S (2012) Multivariate and geostatistical analyses of the spatial distribution and origin of heavy metals in the agricultural soils in Shunyi, Beijing, China. *Sci Total Environ* 425:66–74. <https://doi.org/10.1016/j.scitotenv.2012.03.003>
- Lu X, Zhang X, Li LY, Chen H (2014) Assessment of metals pollution and health risk in dust from nursery schools in Xi'an, China. *Environ Res* 128:27–34. <https://doi.org/10.1016/j.envres.2013.11.007>
- Luo N, An L, Nara A, Yan X, Zhao W (2016) GIS-based multielement source analysis of dustfall in Beijing: a study of 40 major and trace elements. *Chemosphere* 152:123–131. <https://doi.org/10.1016/j.chemosphere.2016.02.099>
- Lyons TJ, Scott WD (1990) Principles of air pollution meteorology. Bellhaven Press, London
- Manno E, Varrica D, Dongarrà G (2006) Metal distribution in road dust samples collected in an urban area close to a petrochemical plant at Gela, Sicily. *Atmos Environ* 40:5929–5941. <https://doi.org/10.1016/j.atmosenv.2006.05.020>
- Manoli E, Voutsas D, Samara C (2002) Chemical characterization and source identification/apportionment of fine and coarse air particles in Thessaloniki, Greece. *Atmos Environ* 36:949–961. [https://doi.org/10.1016/S1352-2310\(01\)00486-1](https://doi.org/10.1016/S1352-2310(01)00486-1)
- Mathur R, Balam V, Satyanarayanan M, Sawant SS (2016) Assessment of heavy metal contamination of road dusts from industrial areas of Hyderabad, India. *Environ Monit Assess* 188:514. <https://doi.org/10.1007/s10661-016-5496-8>
- Mohamed TA, Mohamed MA, Rabeiy R, Ghandour MA (2013) A study of heavy metals in the dust fall around Assiut fertilizer plant. *J Environ Prot* 4:1488–1494. <https://doi.org/10.4236/jep.2013.412170>
- Moreno T, Karanasiou A, Amato F, Lucarelli F, Nava S, Calzolari G, Chiari M, Coz E, Artñano B, Lumberras J, Borge R, Boldo E, Linares C, Alastuey A, Querol X, Gibbons W (2013) Daily and hourly sourcing of metallic and mineral dust in urban air contaminated by traffic and coal-burning emissions. *Atmos Environ* 68:33–44. <https://doi.org/10.1016/j.atmosenv.2012.11.037>
- Muller G (1969) Index of geoaccumulation in sediments of the Rhine River. *GeoJournal* 2:108–118
- Muller G (1981) Die Schwermetallbelastung der sedimentation des Neckars und Seiner Nebenflüsse: Eine Bestandsaufnahme. *Chemiker-Zeitung*, 6:157–164
- Mun'im Mohd Han N, Latif MT, Othman M, Dominick D, Mohamad N, Juahir H, Tahir NM (2014) Composition of selected heavy metals in road dust from Kuala Lumpur city centre. *Environ Earth Sci* 72: 849–859. <https://doi.org/10.1007/s12665-013-3008-5>
- Naddafi K, Nabizadeh R, Soltanianzadeh Z, Ehrampoosh MH (2006) Evaluation of dustfall in the air of Yazd. *Iran J Environ Health Sci Eng* 3:161–168
- Nazzal Y, Ghrefat H, Rosen MA (2014) Application of multivariate geostatistics in the investigation of heavy metal contamination of roadside dusts from selected highways of the Greater Toronto Area, Canada. *Environ Earth Sci* 71:1409–1419. <https://doi.org/10.1007/s12665-013-2546-1>
- Norela S, Nurfatihah MZ, Maimon A, Ismail BS (2009) Wet deposition in the residential area of the Nilai Industrial Park in Negeri Sembilan, Malaysia. *World Appl Sci J* 7:170–179
- Norouzi S, Khademi H, Ayoubi S, Cano AF, Acosta JA (2017) Seasonal and spatial variations in dust deposition rate and concentrations of dust-borne heavy metals, a case study from Isfahan, Central Iran. *Atmos Pollut Res* 8:686–699. <https://doi.org/10.1016/j.apr.2016.12.015>
- Offer ZY, Goossen D (2001) Ten years of Aeolian dust dynamics in a desert region (Negev desert, Israel): analysis of airborne dust events. *J Arid Environ* 47:211–249. <https://doi.org/10.1006/jare.2000.0706>
- Pandey SK, Tripathi BD, Mishra VK (2008) Dust deposition in a subtropical opencast coalmine area, India. *J Environ Manag* 86:132–138. <https://doi.org/10.1016/j.jenvman.2006.11.032>
- Qian Z, He Q, Lin HM, Kong L, Liao D, Dan J, Bentley CM, Wang B (2007) Association of daily cause-specific mortality with ambient particle air pollution in Wuhan, China. *Environ Res* 105:380–389. <https://doi.org/10.1016/j.envres.2007.05.007>
- Ragosta M, Caggiano R, Macchiato M, Sabia S, Trippetta S (2008) Trace elements in daily collected aerosol: level characterization and source identification in a four-year study. *Atmos Res* 89:206–217. <https://doi.org/10.1016/j.atmosres.2008.01.009>
- Reheis MC, Kihl R (1995) Dust deposition in southern Nevada and California, 1984–1989: relations to climate, source area, and source lithology. *J Geophys Res Atmos* 100:8893–8918. <https://doi.org/10.1029/94JD03245>
- Reimann C, Caritat P (2000) Intrinsic flaws of element enrichment factors (EFs) in environmental geochemistry. *Environ Sci Technol* 34: 5084–5091. <https://doi.org/10.1021/es001339e>
- Rout TK, Mastro RE, Padhy PK, George J, Ram LC, Maity S (2014) Dust fall and elemental flux in a coal mining area. *J Geochem Explor* 144: 443–455. <https://doi.org/10.1016/j.gexplo.2014.04.003>
- Salvador P, Artinano B, Alonso DG, Querol X, Alastuey A (2004) Identification and characterization of sources of PM10 in Madrid (Spain) by statistical methods. *Atmos Environ* 38(3):435–447. <https://doi.org/10.1016/j.atmosenv.2003.09.070>
- Schleicher NJ, Norra S, Chai F, Chen Y, Wang S, Cen K, Yu Y, Stüben D (2011) Temporal variability of trace metal mobility of urban particulate matter from Beijing—a contribution to health impact assessments of aerosols. *Atmos Environ* 45:7248–7265. <https://doi.org/10.1016/j.atmosenv.2011.08.067>
- Shah MH, Shaheen N (2007) Statistical analysis of atmospheric trace metals and particulate fractions in Islamabad, Pakistan. *J Hazard Mater* 147:759–767. <https://doi.org/10.1016/j.jhazmat.2007.01.075>
- Shi G, Chen Z, Bi C, Wang L, Teng J, Li Y, Xu S (2011) A comparative study of health risk of potentially toxic metals in urban and suburban road dust in the most populated city of China. *Atmos Environ* 45: 764–771. <https://doi.org/10.1016/j.atmosenv.2010.08.039>
- Soltani N, Keshavarzi B, Moore F, Tavakol T, Lahijanazadeh AR, Jaafarzadeh N, Kermani M (2015) Ecological and human health hazards of heavy metals and polycyclic aromatic hydrocarbons (PAHs) in road dust of Isfahan metropolis, Iran. *Sci Total Environ* 505:712–723. <https://doi.org/10.1016/j.scitotenv.2014.09.097>
- Sutherland RA (2000) Bed sediment-associated trace metals in an urban stream, Oahu, Hawaii. *Environ Geol* 6:611–627. <https://doi.org/10.1007/s002540050473>
- Ta W, Xiao H, Qu J, Xiao Z, Yang G, Wang T, Zhang X (2004) Measurements of dust deposition in Gansu Province, China, 1986–2000. *Geomorphology* 57:41–51. [https://doi.org/10.1016/S0169-555X\(03\)00082-5](https://doi.org/10.1016/S0169-555X(03)00082-5)
- Tang R, Ma K, Zhang Y, Mao Q (2013) The spatial characteristics and pollution levels of metals in urban street dust of Beijing, China. *Appl Geochem* 35:88–98. <https://doi.org/10.1016/j.apgeochem.2013.03.016>
- Taylor SR, McLennan SM (1985) The continental crust: its composition and evolution. Blackwell Scientific, Oxford
- Thakur M, Deb MK, Imai S, Suzuki Y, Ueki K, Hasegawa A (2004) Load of heavy metals in the airborne dust particulates of an urban city of Central India. *Environ Monit Assess* 95:257–268. <https://doi.org/10.1023/B:EMAS.0000029907.96562.af>
- Tiwari S, Thomas A, Rao P, Chate DM, Soni VK, Singh S, Ghude SD, Singh D, Hopke PK (2018) Pollution concentrations in Delhi India during winter 2015–16: a case study of an odd-even vehicle strategy. *Atmos Pollut Res* 9:1137–1145. <https://doi.org/10.1016/j.apr.2018.04.008>
- Trujillo-González JM, Torres-Mora MA, Keesstra S, Brevik EC, Jiménez-Ballesta R (2016) Heavy metal accumulation related to population density in road dust samples taken from urban sites under

- different land uses. *Sci Total Environ* 553:636–642. <https://doi.org/10.1016/j.scitotenv.2016.02.101>
- Turner A (2011) Oral bioaccessibility of trace metals in household dust: a review. *Environ Geochem Health* 33:331–341. <https://doi.org/10.1007/s10653-011-9386-2>
- US EPA (1989) Risk assessment guidance for superfund, vol. I: human health evaluation manual. EPA/540/1-89/002. Office of Solid Waste and Emergency Response
- US EPA (1996) Soil screening guidance: technical background document. EPA/540/ R-95/128. Office of Solid Waste and Emergency Response
- US EPA (2001) Supplemental guidance for developing soil screening levels for superfund sites. OSWER 9355.4–24. Office of Solid Waste and Emergency Response
- US EPA (2002a) Calculating upper confidence limits for exposure point concentrations at hazardous waste sites. OSWER 9285.6-10. Washington, DC: Office of Emergency and Remedial Response, U.S. Environmental Protection Agency. 20460
- US EPA (2002b) Child specific exposure factors handbook. EPA-600-P-00-002B. National Center for Environmental Assessment, Washington, DC
- US EPA (2007) Estimation of relative bioavailability of lead in soil and soil-like materials using in vivo and in vitro methods. OSWER 9285.7–77. Office of Solid Waste and Emergency Response, U.S. Environmental Protection Agency, Washington, DC
- US EPA (2010) Region 9, Regional screening levels tables
- US EPA (2011) Exposure factors handbook 2011 edition. EPA/600/R-09/052F. National Center for Environmental Assessment, Office of Research and Development, U.S. Environmental Protection Agency, Washington, D.C., p 20460
- Van den Berg R (1994) Human exposure to soil contamination: a qualitative and quantitative analysis towards proposals for human toxicological intervention values (partly revised edition). RIVM Rapport 725201011
- Wang YF, Huang KL, Li CT, Mi HH, Luo JH, Tsai PJ (2003) Emissions of fuel metals content from a diesel vehicle engine. *Atmos Environ* 37:4637–4643. <https://doi.org/10.1016/j.atmosenv.2003.07.007>
- Wang R, Zou X, Cheng H, Wu X, Zhang C, Kang L (2015) Spatial distribution and source apportionment of atmospheric dust fall at Beijing during spring of 2008–2009. *Environ Sci and Pollut Res* 22:3547–3557. <https://doi.org/10.1007/s11356-014-3583-3>
- Wei B, Yang L (2010) A review of heavy metal contaminations in urban soils, urban road dusts and agricultural soils from China. *Microchem J* 94:99–107. <https://doi.org/10.1016/j.microc.2009.09.014>
- Xiong QL, Zhao WJ, Guo XY, Shu TT, Chen FT, Zheng XX, Gong ZN (2015) Dustfall heavy metal pollution during winter in North China. *Bull Environ Contam Toxicol* 95:548–554. <https://doi.org/10.1007/s00128-015-1611-8>
- Yadav S, Rajamani V (2006) Air quality and trace metal chemistry of different size fractions of aerosols in N–NW India—implications for source diversity. *Atmos Environ* 40:98–712. <https://doi.org/10.1016/j.atmosenv.2005.10.005>
- Yongming H, Peixuan D, Junji C, Posmentier ES (2006) Multivariate analysis of heavy metal contamination in urban dusts of Xi'an, Central China. *Sci Total Environ* 355:176–186. <https://doi.org/10.1016/j.scitotenv.2005.02.026>
- Zhang J, Hua P, Krebs P (2017) Influences of land use and antecedent dry-weather period on pollution level and ecological risk of heavy metals in road-deposited sediment. *Environ Pollut* 228:158–168. <https://doi.org/10.1016/j.envpol.2017.05.029>
- Zhao J, Peng PA, Song J, Ma S, Sheng G, Fu J (2010) Research on flux of dry atmospheric falling dust and its characterization in a subtropical city, Guangzhou, South China. *Air Qual Atmos Health* 3:139–147. <https://doi.org/10.1007/s11869-009-0062-y>
- Zheng N, Liu J, Wang Q, Liang Z (2010) Heavy metals exposure of children from stairway and sidewalk dust in the smelting district, northeast of China. *Atmos Environ* 44:3239–3245. <https://doi.org/10.1016/j.atmosenv.2010.06.002>
- Ziomas IC, Melas D, Zerefos CS, Bais AF, Paliatsos AG (1995) Forecasting peak pollutant levels from meteorological variables. *Atmos Environ* 29:3703–3711. [https://doi.org/10.1016/1352-2310\(95\)00131-H](https://doi.org/10.1016/1352-2310(95)00131-H)

Publisher's note Springer Nature remains neutral with regard to jurisdictional claims in published maps and institutional affiliations.